

Studies of the oxidation of iron by water vapour using X-ray photoelectron spectroscopy and QUASES™

A.P. Grosvenor^{a,b,*}, B.A. Kobe^a, N.S. McIntyre^{a,b}

^a *Surface Science Western, Room G-1, Western Science Centre, The University of Western Ontario, London, Ont., Canada N6A 5B7*

^b *Department of Chemistry, The University of Western Ontario, London, Ont., Canada N6A 5B7*

Received 22 June 2004; accepted for publication 24 August 2004

Available online 15 September 2004

Abstract

The oxidation of Fe by water (H₂O) vapour was studied using X-ray photoelectron spectroscopy (XPS) and QUASES™. The results indicated that the oxide formed at 25 °C and 150 °C was thinner than that formed when oxygen (O₂) gas was present. The kinetics of the reaction were studied and found to follow a direct logarithmic relationship at both 25 °C and 150 °C. At 150 °C, a change in mechanism occurred after an oxide layer of approximately 0.7 nm had formed. It was determined the mechanism changed from a temperature-independent place-exchange to a temperature-dependent field-driven mechanism. The decreased rate of oxide growth in water vapour compared to that in O₂ is proposed to result from the presence of H within the oxide as well as adsorbed to the surface. Its location within the oxide acts to restrict the amount of diffusion that can occur, while its presence on the surface restricts the number of surface states available for further adsorption of H₂O. The slow conversion of hydroxide to oxide, as well as differences in transport properties between hydroxides and oxides, were also felt to decrease the thickness of the layer formed compared to equivalent reactions with oxygen.

© 2004 Elsevier B.V. All rights reserved.

Keywords: X-ray photoelectron spectroscopy; Iron; Water; Oxidation; Tunneling; Polycrystalline surfaces

1. Introduction

The passivation of iron (Fe) by liquid water or water vapour (H₂O) has received great attention in the past; its reaction is found to form a much thin-

ner oxide layer than if the surface was subjected to oxygen gas (O₂) [1–3]. The oxide film formed at ambient temperature has been suggested to contain primarily Fe oxy-hydroxide (FeOOH) [1,4], while at higher temperatures (550 °C), only Fe₂O₃ and Fe₃O₄ have been found to form [5]. Electrochemical experiments performed using a borate buffer solution have also indicated that the oxide formed contains a γ -Fe₂O₃/Fe₃O₄-like phase, but

* Corresponding author. Tel.: +1 519 661 2173/2111; fax: +1 519 661 3709.

E-mail address: agrosven@uwo.ca (A.P. Grosvenor).

with a spinel rather than inverse-spinel structure [6,7]. Temperature programmed desorption (TPD) studies of H₂O on Fe have indicated that the adsorption reaction is as follows: water adsorbs onto the surface of Fe and is transformed to adsorbed hydroxide (OH_(ads)) and hydrogen (H_(ads)), which can undergo further transformation to adsorbed oxygen (O_(ads)) and hydrogen gas (H_{2(g)}) if a temperature above 107 °C is used [8,9]. This can be represented as



The difference in oxide thickness formed during exposure to H₂O compared to O₂ has been suggested to be a result of the presence of adsorbed hydrogen (H_(ads)) hindering further adsorption of H₂O [10]. The reaction kinetics of oxide growth versus exposure have been found to follow direct rather than inverse logarithmic kinetics [10], just as is proposed for the reaction of Fe with O₂ [11,12].

Advances in determining the depth of origin of species in a surface from electron spectra has allowed X-ray photoelectron spectroscopy (XPS) to become an excellent technique for studying the oxidation of metals. Specifically, algorithms developed by Tougaard [13] allow the background due to extrinsic loss from XP spectra to be modelled, therefore determining the depth of origin of the elements and phases of interest. These algorithms have been incorporated into a software package called QUASES™ [14], which contains two programs: “Analyze” and “Generate”. “Analyze” models the extrinsic background of a photoelectron peak, allowing one to determine the range of depth at which the bulk structure originated. “Generate”, on the other hand, allows the experimental spectra to be modelled using various combinations of reference spectra whose extrinsic backgrounds have been altered based on the depth at which they are found within the surface [14,15]. The accuracy of the thickness determined is dependent upon the attenuation length and the energy loss function (inelastic electron scattering cross-section) used. Studies of the oxidation of Fe by O₂ performed in this laboratory using this software have shown that it is able to allow for

the composition of an oxide layer to be decomposed into its individual parts, enabling the kinetics of the different oxides formed to be tracked over time [11].

This paper describes results from oxidation studies of Fe reacted with H₂O vapour at low pressures and different temperatures using a range of exposures far greater than have been used in the past [1–4]. Individual oxides and hydroxides located within the oxide films formed have been identified and their chemistry will be discussed. The effect of increasing H₂O exposure and temperature will also be presented, along with the kinetics of the reaction that were found to follow a direct logarithmic relationship with time. The results will be compared to those found for the reaction of Fe with O₂.

2. Experimental

2.1. Sample preparation

Pure polycrystalline iron rod (99.995%) from Alfa Aesar was cut into 3.4 mm disks using a diamond saw with one surface being polished to a mirror finish using 0.05 μm γ-Al₂O₃. Samples were degreased in methanol using an ultrasonic cleaner and then loaded into a Kratos AXIS Ultra XPS for water vapour treatment and analysis. All samples were cleaned again in the vacuum chamber of the Kratos spectrometer, first by sputter cleaning the surface for 10 min using a 4 kV Ar⁺ ion beam, then by annealing in vacuum at 600 °C for 30 min. After the in vacuo cleaning, all of the samples were analyzed by XPS to confirm that all contaminant species (C, Na, etc.) had been removed and that no surface oxides remained.

2.2. Reactions

To oxidize the clean Fe surface, a solution containing 95% deionized H₂O and 5% D₂O (Alfa Aesar) was used. Any dissolved gases present in the liquid were removed by multiple freeze–pump–thaw cycles. After introduction into the vacuum chamber where the dosing was performed, the Fe samples were exposed to the reactant vapour until

doses of 10^4 to 10^8 Langmuir (L) were reached at temperatures of 25 ± 1 and 150 ± 1 °C. The pressures used were measured using a Pirani gauge and ranged from 1.3×10^{-2} to 1.3 Pa.

The reaction kinetics were observed at an oxygen dosing pressure of 6.5×10^{-2} Pa and temperatures of 25 ± 1 and 150 ± 1 °C. The exposure times were 100, 200, 500 and 2000s. After dosing, the samples were returned to the analytical chamber and analyzed using the following conditions: monochromatic Al K α X-ray source, binding energy (BE) range = 1100–0 eV, step size = 0.7 eV, pass $E = 160$ eV, sweep time = 180s, and number of sweeps = 8. High resolution spectra were also taken for Fe2p, O1s, and C1s using a 20–40 eV window, depending on the peak analyzed, and a pass energy of 40 eV. The transfer lens was used in electrostatic mode due to the ferromagnetic properties of Fe.

2.3. Data analysis

All spectra were first analyzed using the CasaXPS software [16]. Peak shifts due to any apparent charging were normalized with the C 1s peak set to 284.8 eV. The Fe2p high resolution spectra were fitted using Gupta–Sen multiplet peaks [11,17–19] to determine the presence of different Fe $^{2+}$ and Fe $^{3+}$ oxide/hydroxide species.

High resolution O 1s spectra were also analyzed to determine the presence of oxide/hydroxide species. O 1s binding energies are among the most confusing to assign because of the proximity in BE of many surface and bulk species that have different chemical states. In the case of oxide species on iron surfaces, the O 1s spectra can be compared for oxidation conditions with and without the presence of H $_2$ O. In Fig. 1, the O 1s spectra are compared for exposures of pure Fe to 10^4 L of O $_2$ (Fig. 1a) and 10^4 L of H $_2$ O vapour (Fig. 1b) at ambient temperature. In the case of the O $_2$ exposure, the concentration of H $_2$ O was so low ($P_{\text{H}_2\text{O}}/P_{\text{O}_2} < 10^{-4}$) that the presence of OH species could be eliminated as contributing to the O 1s spectra. Both of the spectra show a peak at 530.0 ± 0.1 eV corresponding to lattice O $^{2-}$ from FeO, Fe $_3$ O $_4$, FeOOH etc. [1,21]. The next highest O 1s peak in the spectra of the O $_2$ exposed surface, found at a BE of $531.6 \text{ eV} \pm 0.1$ eV, is attributed to adsorbed atomic oxygen (O $_{(\text{ads})}$) [11]. From angular-dependent measurements, this peak was shown to be associated with the outer surface. Concerning the O 1s spectrum of the H $_2$ O exposed surface, the peak located at 531.3 ± 0.1 eV (next to the lattice O $^{2-}$ peak) represents the OH $^-$ contribution from Fe(OH) $_2$, and FeOOH [1]. The peak at the next highest binding energy, centred at 532.1 ± 0.1 eV, is attributed to adsorbed OH (OH $_{(\text{ads})}$) located on the Fe surface after oxidation

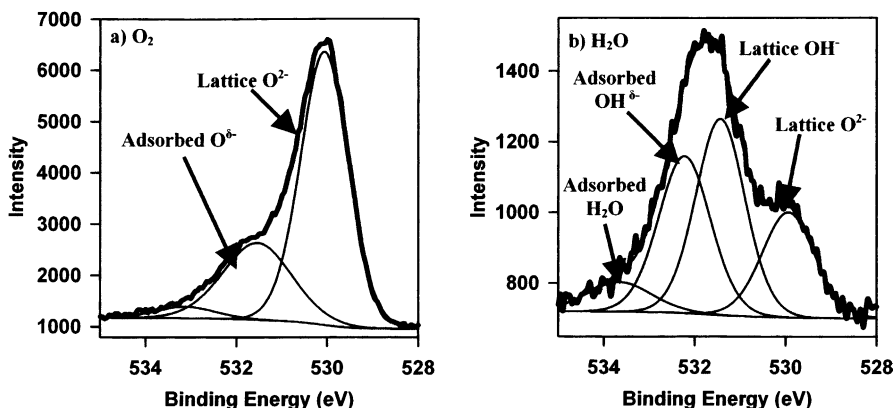


Fig. 1. High resolution O 1s spectra after exposure of a clean Fe surface to O $_2$ (a) and H $_2$ O vapour (b) at ambient temperature indicating the different chemical species found. Both exposures had a total dose of 10^4 L. The O 1s results for the exposure of O $_2$ to Fe come from Ref. [11].

in H₂O vapour. In terms of the adsorbed O and OH species, it is believed that although these species would adsorb as atomic (O) or molecular (OH) species, they would receive a partial negative charge from tunnelling electrons from the metal to the surface, as has been suggested to occur during the oxidation of Fe [22]. For this reason, O_(ads) and OH_(ads) are better represented as O_{(ads)^{δ-}} and OH_{(ads)^{δ-}}. The partial negative charge would allow these species to have an O 1s BE near those found for lattice O²⁻ and OH⁻. The final peak present in the O 1s spectrum of the H₂O exposed surface represents adsorbed H₂O, and was found to have a binding energy of 533.3 ± 0.3 eV. The increased concentration of adsorbed OH_{(ads)^{δ-}} present, compared to adsorbed H₂O in Fig. 1b, supports the adsorption reaction of H₂O on Fe presented in the introduction.

To determine the approximate oxide layer depth, QUASES™ Analyze was used to assess the oxide thickness from the O 1s extrinsic loss structure. The attenuation lengths (λ) used in the QUASES™ computations were approximated by inelastic mean free path (IMFP) values determined using the TPP-2M equation [23]; these were then modified using the same factor indicated in Refs. [11,15]. The modification was based on comparative analyses performed on a stable oxide layer formed on Fe using nuclear reaction analysis (NRA) and XPS using QUASES™ to analyze the data [15]. The results indicated that the oxide thickness determined using QUASES™ was 20% greater than the value determined by NRA, which was attributed to the difference between the IMFP used and the true attenuation length [15]. The attenuation length value for O 1s was determined using Fe₃O₄ as the model compound and a kinetic energy of 956 eV. The attenuation length ($\lambda_{\text{O}1\text{s}}$) was determined to be 1.6 nm. The universal cross-section developed by Tougaard [24] was used for all species analyzed.

QUASES™ Generate was used to determine the depth of individual oxide layers using the Fe 2p region on the basis of the appropriate reference spectra obtained during previous studies. Reference samples used were the same as those discussed in Ref. [15], with a spectrum from Fe(OH)₂ also being used. The Fe(OH)₂ sample was synthesized

by precipitating a hot solution of FeCl₂ with NaOH under the cover of Ar gas [25]. Spectra from the reference compounds were all used either separately or in combination to model the experimental spectra under consideration. The surfaces were always modelled in such a way that the Fe metal spectra remained as the bulk, overlaid by Fe²⁺ compounds, followed by Fe³⁺ compounds (if present). A spectrum was deemed to have been adequately fitted if the model spectra almost or completely overlaid the extrinsic background region of the experimental spectra located between kinetic energies of 720 and 750 eV. An example of the model spectra found using various combinations of reference spectra and QUASES™ Generate is shown in Fig. 2. Further information on the methodology used when fitting the spectra using either Generate or Analyze can be found in Ref. [15]. The attenuation length values used for the Fe 2p photoelectrons from the metal and oxides were: $\lambda_{\text{Fe}} = 1.3$ nm, $\lambda_{\text{FeO}} = 1.3$ nm, $\lambda_{\text{Fe(OH)}_2} = 1.3$ nm, $\lambda_{\text{Fe}_3\text{O}_4} = 1.4$ nm, $\lambda_{\text{Fe}_2\text{O}_3} = 1.4$ nm, and $\lambda_{\text{FeOOH}} = 1.4$ nm.

2.4. Results

2.4.1. Effects of H₂O dose: 25 °C and 150 °C

Fe 2p_{3/2} high resolution spectra obtained after clean Fe surfaces were oxidized by H₂O at a temperature of 25 °C with exposure levels ranging from 10⁴ to 10⁸ L are shown in Fig. 3a–c. The extent of oxidation found at this temperature is low, with the oxide portion of the spectra requiring careful fitting to differentiate it from the very strong Fe metal peak, particularly after a dose of only 10⁴ L. The oxides produced after the lowest level of exposure to H₂O were found to contain Fe²⁺ species only based on the multiplet structure observed (see inset in Fig. 3a) [20]. Following higher doses, peaks associated with both Fe²⁺ and Fe³⁺ species were found. The O 1s high resolution spectra shown in Fig. 3d–f indicate that at ambient temperature (25 °C), the surface film contained primarily OH⁻ at the lowest exposure (10⁴ L); with increased exposure, the lattice oxygen component (O²⁻) became dominant. Angle-resolved studies indicated that the concentration of OH⁻ increased compared to that of O²⁻ with decreasing electron take-off angle; this

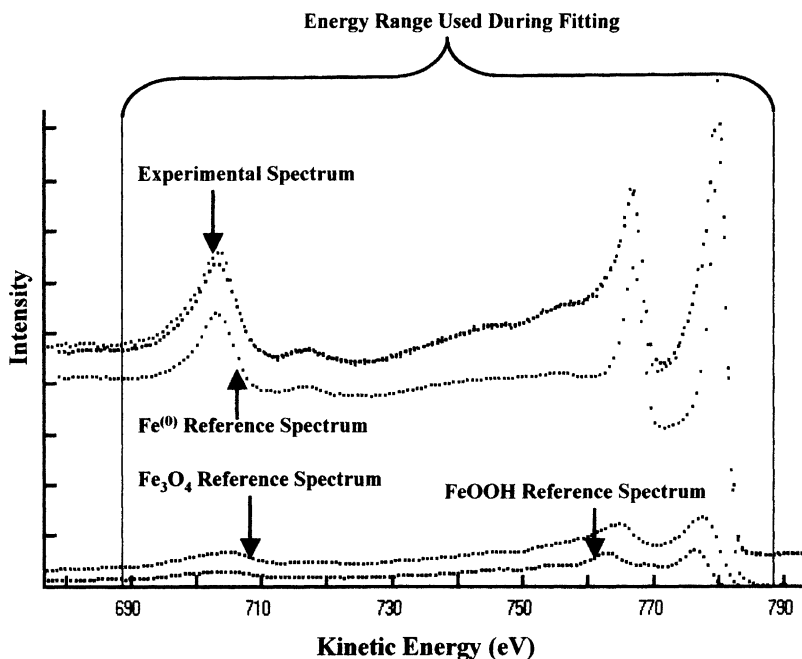


Fig. 2. QUASES™ Generate Fe2p model of an Fe surface exposed to 10^8 L H_2O at $25^\circ C$. The model spectrum was found to completely overlay the experimental spectrum for the energy range of 710 eV to 790 eV (kinetic energy). The spectrum indicated here corresponds to the model shown in Fig. 4c.

indicates that the reactive hydroxide species lies on top of the oxide. After additional dosing with water, some of this hydroxide is transformed into an oxide by losing H after further reaction with Fe metal. All of the O 1s high resolution spectra also indicated the presence of significant amounts of adsorbed $OH_{(ads)}^-$ (532.1 ± 0.1 eV) and adsorbed H_2O (533.3 ± 0.3 eV), in accord with the adsorption reaction presented in the Introduction.

Fig. 4a–c show the QUASES™ Generate derived oxide thicknesses and compositions following a series of H_2O doses at $25^\circ C$. After an exposure of 10^4 L at $25^\circ C$, the outermost surface consists of $Fe(OH)_2$ with an underlying layer of FeO. The ferrous nature of the oxide could also be inferred from the spectral deconvolution shown in Fig. 3a. Exposures to higher doses of H_2O show that the surface layer consists of FeOOH with an underlying layer of Fe_3O_4 ; at these higher doses no FeO or $Fe(OH)_2$ could be detected. The models also show a considerable quantity of metallic iron present within the oxide layers at low doses; this is probably associated with portions of unreacted

metal grains. The amount of metal within the oxide was found to decrease as the dose increased. The analysis provided by QUASES™ Generate has, for the first time, allowed the detailed compositions of oxidation products to be determined for the initial reaction of iron with water vapour.

The $Fe 2p_{3/2}$ spectra from the experiments performed at $150^\circ C$ are shown in Fig. 5a–c. At $150^\circ C$, Fe^{2+} species form at the lowest dose, while species containing both Fe^{2+} and Fe^{3+} formed after higher exposures. The O 1s spectra from the reactions at $150^\circ C$ shown in Fig. 5d–f indicate that the dominant oxygen species is lattice oxide (O^{2-}) throughout the exposure range, and that the ratio of $O^{2-}:OH^-$ in the surface oxide layer increases with dose. These results confirm those found by Hultquist et al. [26] for similar reactions that also showed that with increasing reaction temperature, the concentration of O^{2-} in the oxide film increased while the concentration of OH^- decreased. All of the O 1s spectra shown in Fig. 5d–f were also found to contain a peak at 531.6 ± 0.1 eV associated with adsorbed oxygen on the surface

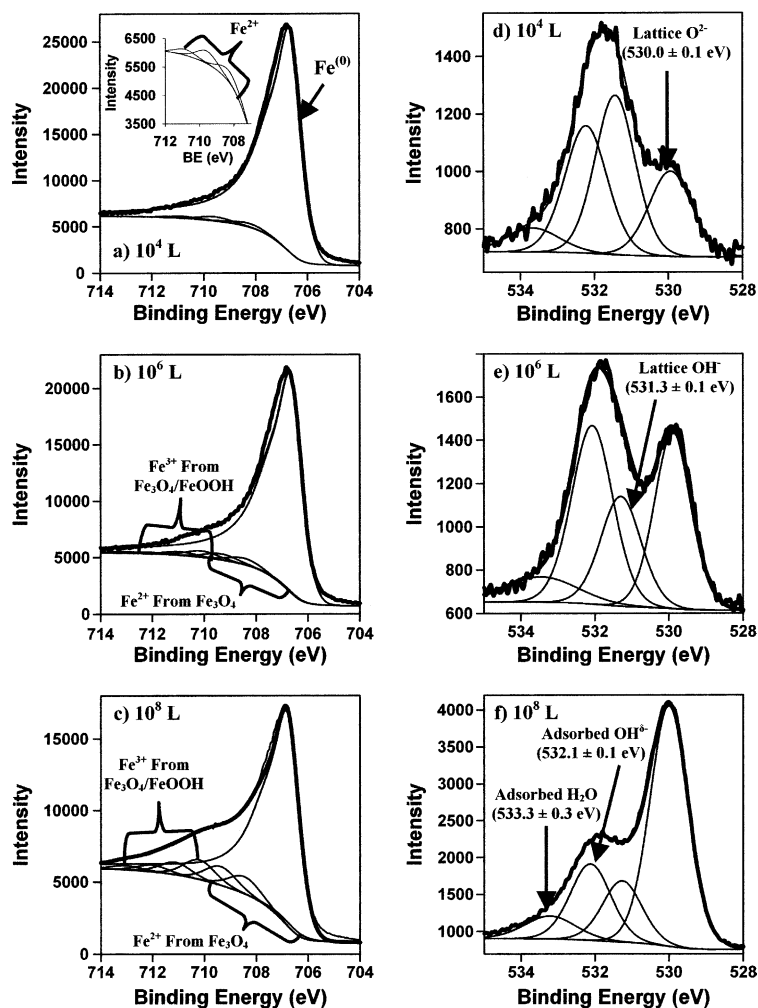


Fig. 3. Fe $2p_{3/2}$ and O1s high resolution spectra after oxidation by H $_2$ O at 25°C: (a) Fe $2p_{3/2}$, 10^4 L; (b) Fe $2p_{3/2}$, 10^6 L; (c) Fe $2p_{3/2}$, 10^8 L; (d) O1s, 10^4 L; (e) O1s, 10^6 L; (f) O1s, 10^8 L. All Fe $2p_{3/2}$ spectra have been fit using Gupta–Sen multiplet peaks representing Fe $^{2+}$ and Fe $^{3+}$ species as well as the metal peak which is represented by an asymmetric peak.

(O $_{(ads)}^{\delta-}$); this was not observed in the O1s spectra from the reactions performed at 25°C. The concentration of O $_{(ads)}^{\delta-}$ was found to increase with increasing dose.

The thicknesses and identity of the films formed at 150°C determined using QUASES™ Generate are shown in Fig. 4d–f. At the lowest dose, the film was found to contain Fe(OH) $_2$ overlaying a layer of FeO like that formed during the reaction performed at 25°C. At higher doses, however, the oxide layers were found to consist of Fe $_3$ O $_4$ covered by FeOOH after receiving a dose of 10^6 L

and Fe $_3$ O $_4$ covered by a layer that was intermediate between FeOOH and Fe $_2$ O $_3$ after receiving a dose of 10^8 L. The Fe $^{3+}$ layer found after the highest dose could not be identified as containing either FeOOH or Fe $_2$ O $_3$ based on the QUASES™ fittings. The oxide thickness was found to increase much more rapidly at 150°C than at 25°C.

2.4.2. Oxidation kinetic studies at two temperatures

The range of H $_2$ O pressures over which this study was conducted was restricted compared to that used in a previous O $_2$ oxidation study [11].

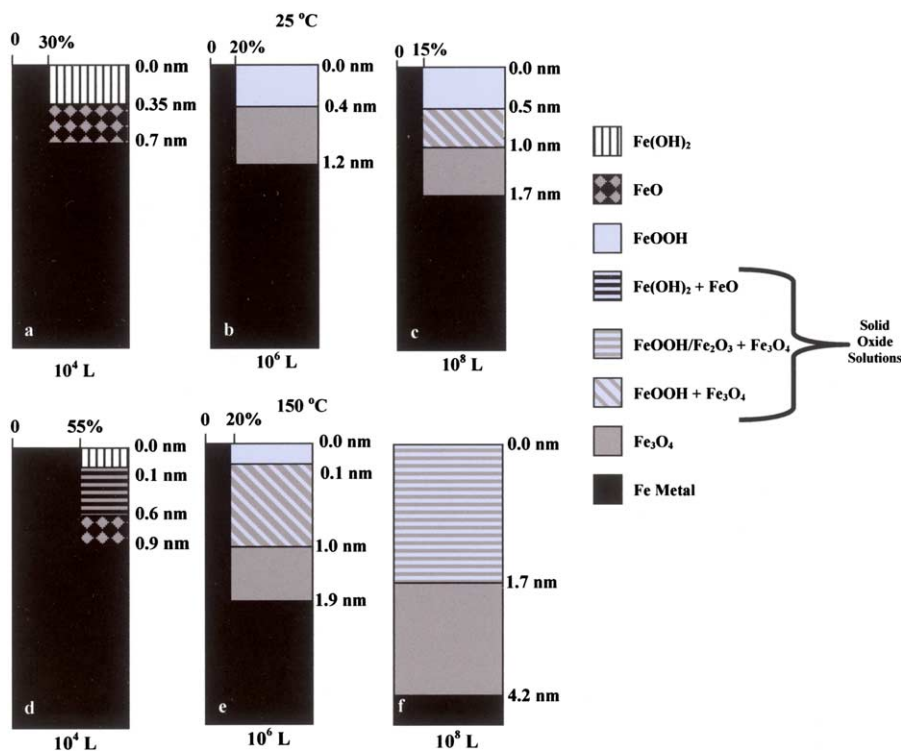


Fig. 4. Profiles of oxide thicknesses and compositions determined using QUASES™ Generate for samples exposed to H₂O using the following conditions: (a) 10⁴L, 25°C; (b) 10⁶L, 25°C; (c) 10⁸L, 25°C; (d) 10⁴L, 150°C; (e) 10⁶L, 150°C; (f) 10⁸L, 150°C.

Consequently, any pressure effects on the oxide growth kinetics, such as those observed in the O₂ study, could not be followed here. The effect of H₂O dose on oxide thickness is plotted in Fig. 6 using the thickness measurements derived from QUASES™ Analyze and the O 1s spectra. Comparable overall thicknesses were obtained from QUASES™ Generate and the Fe 2p spectra. The relationship between oxide thickness and H₂O dose in the pressure range (1.3×10^{-2} – 1.3 Pa) studied was found to be best fitted by a direct logarithmic function for both temperatures. The increase of slope for the reaction at 150 °C compared to the reaction at 25 °C provides a good measure of the increased reactivity at this temperature.

Using a constant reaction pressure of $(6.5 \pm 0.1) \times 10^{-2}$ Pa, the rate of oxide growth was determined as a function of time at 25 °C and 150 °C (see Fig. 7). Kinetic results from an earlier oxidation study of Fe using O₂ at 27 °C [11] have also been included in the figure. Both reac-

tions (O₂ and H₂O) were best fitted using a direct logarithmic function with increasing time. The thicknesses found for the oxides formed using H₂O were much less than those formed using O₂, even when the reaction temperature was increased. The slopes of the plots for the H₂O reaction at 150 °C and the O₂ reaction at 27 °C are similar; this would suggest that the diffusion mechanisms are similar. In both cases, the overwhelming medium for diffusion is oxide, not hydroxide.

The kinetic curves found in Fig. 7 for the reactions performed at 25 °C and 150 °C intersect at a time near 100 s. This was investigated further by oxidizing two Fe disks with H₂O vapour at 25 °C and 150 °C for 50 s at 6.5×10^{-2} Pa (dose $\approx 2.5 \times 10^4$ L). The oxide thicknesses formed were the same (0.7 nm) and had similar compositions: FeO overlaid by Fe(OH)₂. These overlying results, included in Fig. 7, show that the iron–water vapour reaction has a different response to temperature at this early stage. Effectively, this

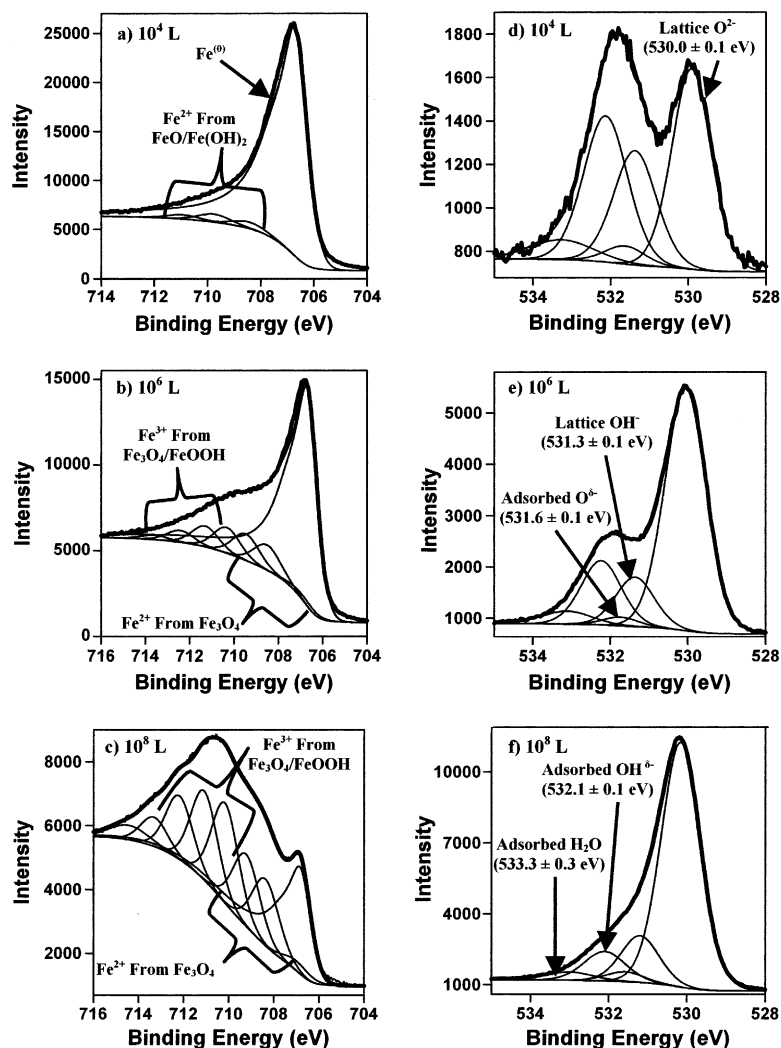


Fig. 5. Fe $2p_{3/2}$ and O1s high resolution spectra after oxidation by H $_2$ O at 150°C: (a) Fe $2p_{3/2}$, 10 4 L; (b) Fe $2p_{3/2}$, 10 6 L; (c) Fe $2p_{3/2}$, 10 8 L; (d) O1s, 10 4 L; (e) O1s, 10 6 L; (f) O1s, 10 8 L. All Fe $2p_{3/2}$ spectra have been fit using Gupta–Sen multiplet peaks representing Fe $^{2+}$ and Fe $^{3+}$ species as well as the metal peak which is represented by an asymmetric peak.

suggests different oxidation mechanisms for the reaction of Fe with H $_2$ O vapour at 150°C before and after an oxide layer around 0.7 nm thick had formed.

3. Discussion

The extended oxidation of Fe is proposed to begin with electrons tunnelling through an existing thin oxide layer to establish an electric field to

drive further growth [22]. The initial thin oxide layer is believed to form via place-exchange and to have a thickness of only one to two mono-layers [11,27,28]. In this particular study, any place-exchange would involve adsorbed hydroxyl groups with an expected high free energy of activation. As a result, this step would occur slowly. By contrast, when atomic oxygen is the primary adsorbate (as in the reaction of O $_2$ with Fe) the place-exchange step would be expected to involve a lower free energy of activation. In the case of the water vapour

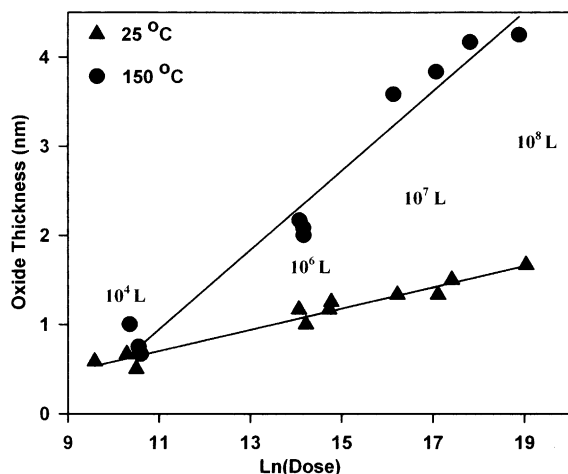


Fig. 6. Relationships between log H₂O dose and oxide thickness as determined by QUASES™ Analyze for the reaction of polycrystalline Fe with water vapour. Results for the reactions studied at both 25 °C and 150 °C are shown.

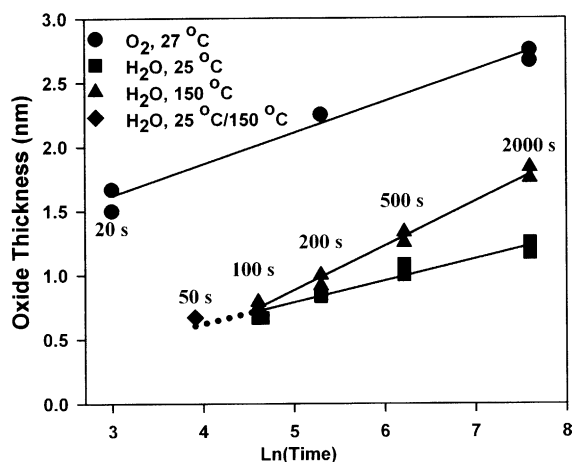


Fig. 7. Kinetic results found using QUASES™ Generate for reactions involving H₂O at 25 °C and 150 °C for the reaction times indicated. Doses used during the kinetic study ranged from 10⁴ to 10⁶ L. Kinetic results found for the reaction involving O₂ from Ref. [11] have also been included. All results were found to be best fitted using a direct logarithmic relationship (x versus $\ln(t)$). Fittings performed using an inverse logarithmic function ($1/x$ versus $\ln(t)$) gave R^2 values that were significantly less. The results from the reactions performed at 25 °C and 150 °C for 50 s showing identical thicknesses have also been included.

reaction, a large concentration of atomic hydrogen resulting from scission of adsorbed water may also

retard the growth rate of the film, both during place-exchange and during the subsequent field-driven growth [1,10], by blocking surface states normally available for adsorption. The apparent slow conversion of the hydroxide to an oxide during the reaction of H₂O vapour with Fe will produce additional hydrogen within the oxide layer—some of which could act to block ion diffusion [4]. Past studies have also suggested that the presence of Fe³⁺ in the oxides formed upon reaction of Fe with H₂O is responsible for the decreased reaction rate observed compared to the reaction of Fe with O₂ [4]. Research performed in this laboratory on the kinetics of the reaction of Fe with O₂ [11] showed that oxides containing Fe³⁺ formed, but the observed oxide thicknesses were still much larger than those observed for the reaction with H₂O (see Fig. 7); this suggests that Fe³⁺ does not restrict the oxidation of Fe.

The increase in rate observed for the reaction of water vapour and Fe at 150 °C (after an oxide thickness of ~0.7 nm had formed) could correspond to the point where the reaction mechanism changes from place-exchange to the field-driven mechanism. This is substantiated by the fact that the thickness of a mono-layer of Fe(OH)₂ is 0.5 nm [29]; only slightly thinner than the oxide layer found to form after an exposure of 50 s at both temperatures (0.7 nm). The place-exchange mechanism appears to be temperature-independent, while the field-driven mechanism shows temperature-dependence.

At 150 °C, and higher doses of water vapour, the population of surface adsorbates will contain increasing concentrations of O_(ads)^{δ-}, and therefore less H will be available within the oxide layer, thus decreasing its ability to block diffusion. The oxide growth rate therefore increases, compared to that at 25 °C. The overall increased reactivity of O_(ads)^{δ-} compared to OH_(ads)^{δ-} also leads to larger concentrations of oxidic structures forming (Fig. 4d–f) whose transport properties should allow more rapid growth compared to hydroxide structures. The increased removal of H from the surface as H_{2(g)} at high temperature also increases the number of surface states available for adsorption of H₂O, which would allow for a thicker oxide to form [10]. The increased size of this layer can also

be attributed to an increase in the electric field by the addition of thermionic emission, which is known to occur at temperatures near 150 °C [30].

All of the oxide layers investigated during the study of the reaction at 150 °C contained substantial amounts of a solid oxide solution. The growth of this solution is attributed to anion diffusion of oxygen through interstitial sites and grain boundaries such as was found for reactions involving O₂ [11]. The dominant diffusion mechanism present at both reaction temperatures is felt to be cation diffusion through vacancies, just as was found for the reaction of Fe with O₂ [11].

The reactions between H₂O and Fe occurring at 25 °C and 150 °C follow a direct logarithmic function with time above exposure times of 50 s. The oxidation of Fe by O₂ has been found to be well described by the kinetic equation proposed by Eley and Wilkinson [11] for mechanisms involving electron tunnelling, and has been used in this study to calculate the reaction rates found for all of the measured reaction times. The equation is presented as follows:

$$\frac{dx}{dt} = aP^{0.6}e^{-bx} = Ae^{-\frac{E}{RT}}P^{0.6}e^{-\frac{\gamma x}{RT}} \quad (1)$$

where A = the pre-exponential value, E = activation energy, P = reaction pressure, T = temperature, x = thickness of the oxide at time t , and γ = increase in activation free energy with increase in thickness of the oxide film [27]. The calculated rates for both reactions, shown in Fig. 8, indicate that the rates for the reaction performed at 150 °C are considerably higher than for the 25 °C reaction for all times shown. As can be seen, the rate of oxide growth decelerates in an exponential fashion for both temperatures as the oxide thickness increases. This result indicates the difficulty in sustaining an electric field across the oxide layer that is capable of supporting further oxidation as the thickness of the layer increases. A similar observation was observed for the reaction of Fe with O₂, but the initial rates found for this reaction were much greater [11]. The presence of hydrogen within the oxide film and adsorbed to the surface, as well as the slow conversion of hydroxide to oxide, are factors responsible for the decrease in the initial reaction rates compared to the O₂ results.

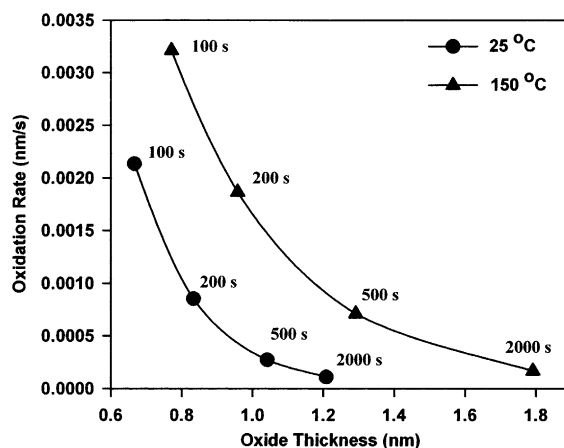


Fig. 8. Reaction rates calculated for the two H₂O reactions studied (25 °C and 150 °C) using Eq. (1) for exposure times ranging from 100 to 2000 s. The results indicate that for both reactions, the rates decelerate exponentially as the oxide thickness increases.

A comparison of the oxide structures produced by low doses (10⁴L) of H₂O and O₂ at ambient temperature indicate that different oxide structures are produced on clean metallic Fe. Water vapour exposure results in the structure shown in Fig. 4a: Fe(OH)₂ on FeO with a thickness of 0.7 nm. An equivalent dose of O₂ on clean Fe, however, results in a layer of γ -Fe₂O₃ on Fe₃O₄ that is 1.7 nm thick [11]. The much slower initial growth rate of the oxide in water vapour must be associated with the character of the Fe(OH)₂/FeO and FeOOH/Fe₃O₄ (formed after higher exposures) structures. It is not clear, however, whether the lower growth rate results from the slow conversion of hydroxide to oxide, the presence of hydrogen adsorbed to the surface or in vacancies/interstitial spaces blocking diffusion sites, or an intensive property of the hydroxide species alone.

4. Conclusion

The oxidation of Fe by water vapour has been investigated using XPS and QUASES™ over a large range of exposures at temperatures of 25 °C and 150 °C. The overall reaction at both temperatures was found to follow direct logarithmic kinetics. The initial nucleation and growth of the hydroxide/oxide film was found to be much slower

than for equivalent reactions of Fe with O₂. This is attributed to a slow place-exchange reaction between adsorbed OH_(ads)^{δ-} and the iron substrate that was found to be independent of temperature. Upon exposure to higher doses of H₂O, the reaction was found to be temperature-dependent and to follow an electric field-driven mechanism. The initial rate of oxide growth compared to the reaction performed using O₂ was lower, with the difference being attributed to the presence of H within the oxide, restricting ion diffusion. The presence of adsorbed H causing a reduction in the number of surface sites available for H₂O to adsorb to as well as the slow conversion of hydroxide to oxide were also believed to cause a decrease in the initial reaction rate compared to the reaction involving O₂.

Acknowledgments

The authors would like to acknowledge the Natural Sciences and Engineering Research Council of Canada (NSERC) for funding this work. Dr. R.St.C. Smart is also thanked for fruitful discussions had during this research.

References

- [1] M.W. Roberts, P.R. Wood, *J. Electron Spectrosc. Relat. Phenom.* 11 (1977) 431.
- [2] J.K. Gimzewski, B.D. Padalia, S. Affrossman, L.M. Watson, D.J. Fabian, *Surf. Sci.* 62 (1977) 386.
- [3] P.A. Lee, K.F. Stork, B.L. Maschhoff, K.W. Nebesny, N.R. Armstrong, *Surf. Interf. Anal.* 17 (1991) 48.
- [4] S.J. Roosendaal, J.P.R. Bakker, A.M. Vredenberg, F.H.P.M. Habraken, *Surf. Sci.* 494 (2001) 197.
- [5] D. Caplan, M. Cohen, *Corros. Sci.* 7 (1967) 725.
- [6] M.F. Toney, A.J. Davenport, L.J. Oblonsky, M.P. Ryan, C.M. Vitus, *Phys. Rev. Lett.* 79 (1997) 4282.
- [7] A.J. Davenport, L.J. Oblonsky, M.P. Ryan, M.F. Toney, *J. Electrochem. Soc.* 147 (2000) 2162.
- [8] W.H. Hung, J. Schwartz, S.L. Bernasek, *Surf. Sci.* 294 (1993) 21.
- [9] H.J. Grabke, *Mater. Sci. Forum* 154 (1994) 69.
- [10] B.L. Maschhoff, N.R. Armstrong, *Langmuir* 7 (1991) 693.
- [11] A.P. Grosvenor, B.A. Kobe, N.S. McIntyre, *Surf. Sci.* 565 (2004) 151.
- [12] M.J. Graham, S.I. Ali, M. Cohen, *J. Electrochem. Soc.* 117 (1970) 513.
- [13] S. Tougaard, *Surf. Interf. Anal.* 26 (1998) 249.
- [14] S. Tougaard, QUASES™, Version 4.4, Software for Quantitative XPS/AES of Surface Nano-Structures by Analysis of the Peak Shape and Background, 2000.
- [15] A.P. Grosvenor, B.A. Kobe, N.S. McIntyre, S. Tougaard, W.N. Lennard, *Surf. Interf. Anal.* 36 (2004) 632.
- [16] N. Fairley, CasaXPS Version 2.2.19, 1999–2003.
- [17] R.P. Gupta, S.K. Sen, *Phys. Rev. B* 10 (1974) 71.
- [18] R.P. Gupta, S.K. Sen, *Phys. Rev. B* 12 (1975) 15.
- [19] N.S. McIntyre, D.G. Zetaruk, *Anal. Chem.* 49 (1977) 1521.
- [20] A.P. Grosvenor, B.A. Kobe, M.C. Biesinger, N. S. McIntyre, *Surf. Interf. Anal.*, in press.
- [21] C.R. Brundle, T.J. Chuang, K. Wandelt, *Surf. Sci.* 68 (1977) 459.
- [22] N. Cabrera, N.F. Mott, *Rep. Prog. Phys.* 12 (1948–49) 163.
- [23] S. Tanuma, C.J. Powell, D.R. Penn, *Surf. Interf. Anal.* 11 (1988) 577.
- [24] S. Tougaard, *Surf. Interf. Anal.* 11 (1988) 453.
- [25] W. Feitknecht, H. Hani, V. Dvorak, in: J.W. Mitchell, R.C. DeVries, R.W. Roberts, P. Cannon (Eds.), *Reactivity of Solids*, Wiley, New York, 1969, p. 237.
- [26] G. Hultquist, M. Seo, Q. Lu, G.K. Chuah, K.L. Tan, *Appl. Surf. Sci.* 59 (1992) 135.
- [27] D.D. Eley, P.R. Wilkinson, *Proc. R. Soc. London A* 254 (1960) 327.
- [28] F.P. Fehlner, N.F. Mott, in: *Oxidation of Metals and Alloys*, papers presented at a seminar of the American Society for Metals, 17 and 18 October 1970, American Society for Metals, Metals Park, 1971, p. 37.
- [29] R.M. Cornell, U. Schwertmann, *The Iron Oxides: Structures, Properties, Reactions, Occurrence and Uses*, VCH, New York, 1996.
- [30] G.W.R. Leibbrandt, G. Hoogers, F.H.P.M. Habraken, *Phys. Rev. Lett.* 68 (1992) 1947.